

Toward a first-principles description of transverse momentum dependent Drell-Yan production in proton-nucleus collisions

Ivan Vitev, LANL

W. Ke, J. Terry, I.V., ArXiv:2408.10310 (appeared yesterday night)



INSTITUTE for **NUCLEAR THEORY**

INT program: Heavy Ion Physics in the EIC Era (24-2b)
Seattle, WA July 29 – August 3, 2024

Outline of the talk

The plan for today

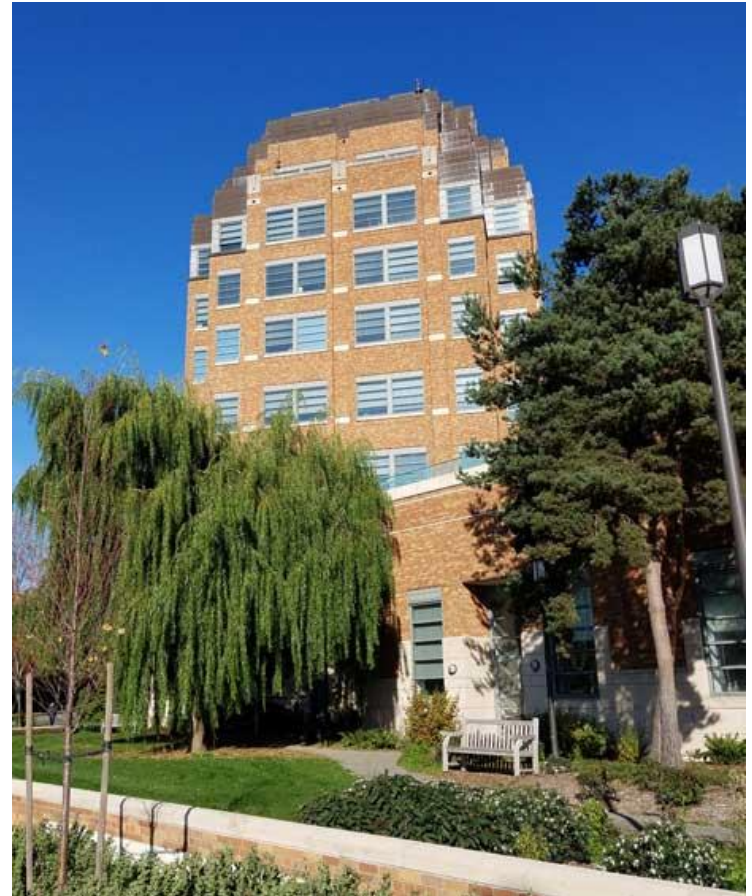
- TMD Physics and the Drell-Yan cross section
- Cold nuclear matter effects in pA, eA
- Computation of the TMD DY cross section in pA reactions and scale analysis
- Collinear, soft, and target sectors of the computation. Cancellation of divergences
- Renormalization, scale and rapidity evolution
- Partial resummation of higher order in opacity contributions
- Phenomenological applications (first try)
- Conclusions

Largely based on the following papers: [2408.10310](#) [hep-ph] (TMD DY); [2301.11940](#) [hep-ph] (RG evolution); [refs therein](#)

- i) Thanks to the INT for hosting this program
- ii) Credit for the work presented goes to my collaborators – for these works W. Ke, J. Terry (+ many others)

For a comprehensive overview of TMD physics “TMD Handbook”

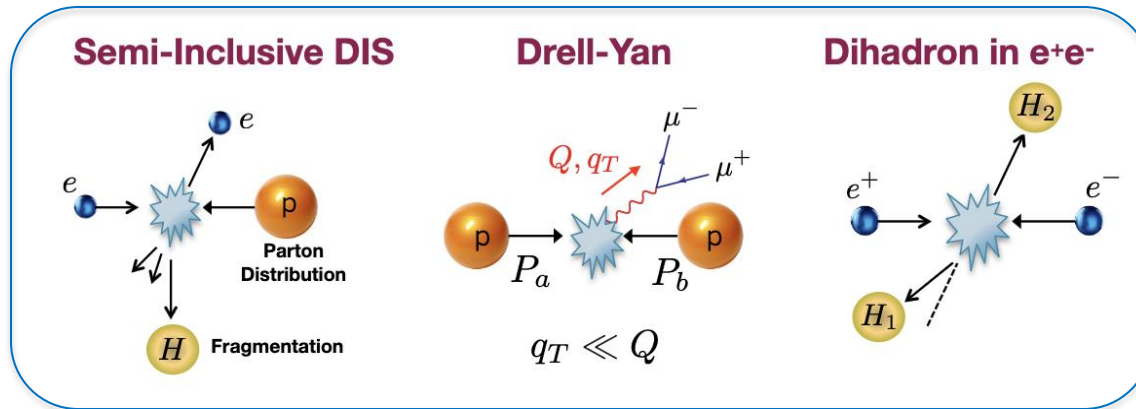
R. Boussarie et al. (2023)



TMD Observables

Transverse Moment Dependent (TMD) observables provide a new window on the non-perturbative structure of hadrons, and nuclei and on fundamental QCD dynamics

- They arise when there is a small transverse momentum in the probe $\Lambda_{\text{QCD}} \lesssim P_T \ll Q$.



- A much more detailed 3D picture of nucleon and nuclear structure
- A better understanding of fragmentation, TMD FFs
- Near back-to-back hadrons, jets, Z/gamma-hadron/jet
- Jet substructure

TMD Handbook

A modern introduction to the physics of Transverse Momentum Dependent distributions



Renaud Boussarie
Matthias Burkardt
Martha Constantinou
William Detmold
Markus Ebert
Michael Engelhardt
Sean Fleming
Leonard Gamberg
Xiangdong Ji
Zhong-Bi Kang
Christopher Lee
Kih-Fei Liu
Simone Lüscher
Thomas Mahen
Andreas Metz
John Nagle
Daniel Pitonyak
Alexei Prokudin
Jan-Willem Qiu
Abhishek Rajan
Marc Schlegel
Phiala Shanahan
Peter Schweitzer
Ian W. Stewart
Andrey Tarasov
Raju Venugopalan
Jian-Vin
Feng Yuan
Yong Zhao
... Editors

R. Boussarie et al. (2023)

| | | Quark Polarization | | |
|----------------------|---|--|--|---|
| | | Un-Polarized (U) | Longitudinally Polarized (L) | Transversely Polarized (T) |
| Nucleon Polarization | U | $f_1 = \odot$ Unpolarized | | $h_1^\perp = \uparrow - \downarrow$ Boer-Mulders |
| | L | | $g_1 = \rightarrow - \leftarrow$ Helicity | $h_{1L}^\perp = \rightarrow - \leftarrow$ Worm-gear |
| Nucleon Polarization | T | $f_{1T}^\perp = \uparrow - \downarrow$ Sivers | $g_{1T}^\perp = \rightarrow - \leftarrow$ Worm-gear | $h_{1T}^\perp = \uparrow - \downarrow$ Transversity $h_{1T}^\perp = \rightarrow - \leftarrow$ Pretzelocity |

Quark TMDs

See. Talk by J. Terry

The Drell-Yan process

Proposed as a new way to study quantum chromodynamics and the structure of the nucleon

S. Drell et al. (1970)

$$\frac{d^2\sigma}{dx_1 dx_2} = \frac{4\pi\alpha}{9x_1 x_2} \sum_{i \in u, d, s, \dots} e_i^2 [q_i^A(x_1) \bar{q}_i^B(x_2) + \bar{q}_i^A(x_1) q_i^B(x_2)]$$

Observed practically immediately in 1970 at the AGS in pU collisions

J. Christenson et al. (1970)

- Used to test sum rules, antiquark flavor asymmetry, search for parton energy loss in pA among others

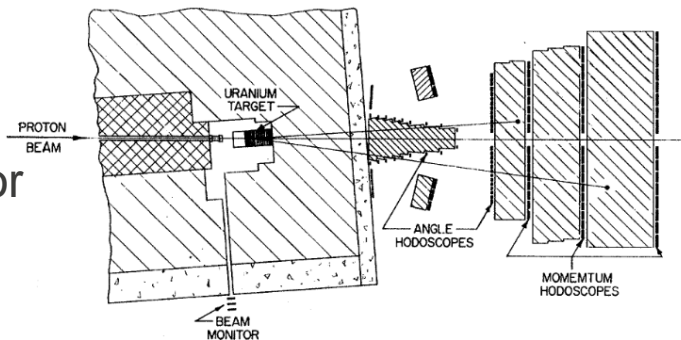
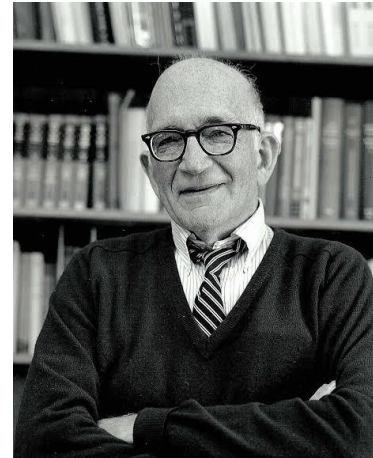
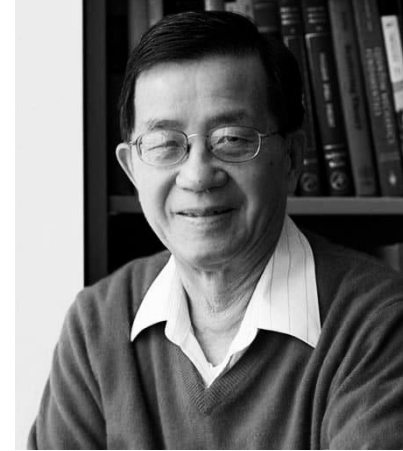


FIG. 1. Plan view of the apparatus.

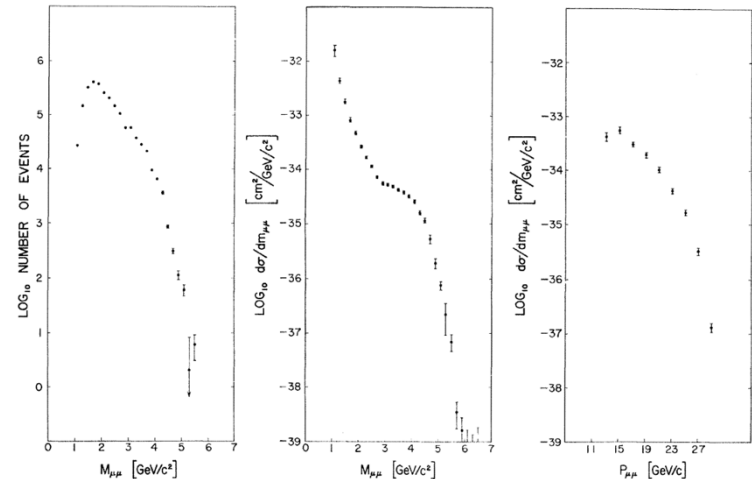
$$\frac{\sigma^{pd}}{2\sigma^{pp}} \approx \frac{1}{2} \left[1 + \frac{\bar{d}(x_2)}{\bar{u}(x_2)} \right]$$



S. Drell



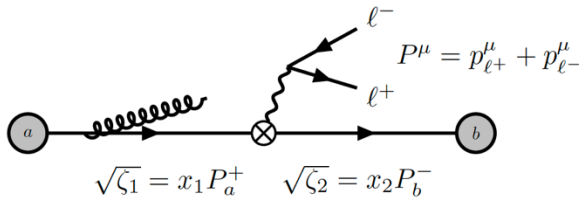
T. Yan



Invariant mass distribution

Factorization in SCET for the TMD DY

**Factorized expression,
impact parameter space**



$$\frac{d\sigma}{dy dQ^2 d^2\mathbf{P}_T} = \sigma_0(Q, \sqrt{s}) H(Q, \mu) \sum_q c_q(Q) \int \frac{d^2\mathbf{b}}{(2\pi)^2} e^{i\mathbf{b}\cdot\mathbf{P}_T} \times \mathcal{B}_{q/a}\left(x_1, b, \mu, \frac{\zeta_1}{\nu^2}\right) \mathcal{B}_{\bar{q}/b}\left(x_2, b, \mu, \frac{\zeta_2}{\nu^2}\right) S(b, \mu, \nu)$$

R. Boussarie et al. (2023)

- Total cross section coefficient (Born level cross section) $\sigma_0(Q, \sqrt{s}) = \frac{4\pi\alpha_{\text{em}}^2}{3N_c Q^2 s}$
- **Hard part** and charge coefficient (only non-trivial when one reaches electroweak scales)
- **Beam function** that matches on the collinear PDF in the perturbative region

$$\mathcal{B}_{q/a}\left(x, b, \mu, \frac{\zeta_1}{\nu^2}\right) = \frac{1}{2N_c} \int \frac{d^4z}{2\pi} e^{iz\cdot p} \delta(n\cdot z) \delta^2(\mathbf{z}_T - \mathbf{b}) \text{Tr} \left[\left\langle P_a \left| \bar{\chi}_n(z) \frac{\not{h}}{2} \chi_n(0) \right| P_a \right\rangle \right]$$

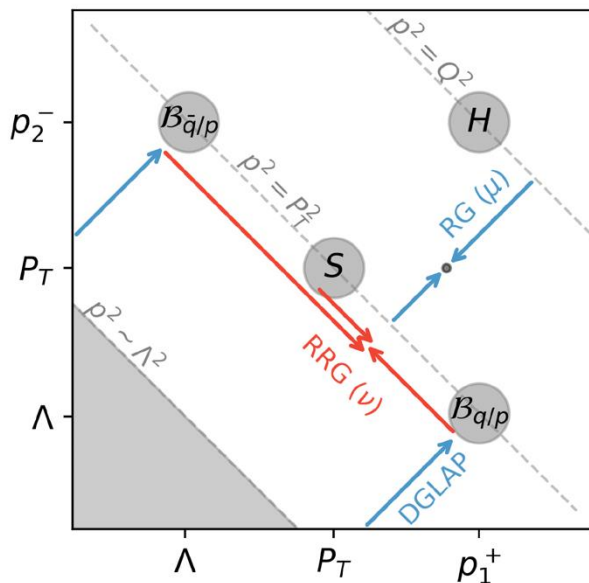
$$\mathcal{B}_{q/a}\left(x_1, b, \mu, \frac{\zeta_1}{\nu^2}\right) = \sum_i \int_{x_1}^1 \frac{dx}{x} C_{q/i}\left(x, b, \mu, \mu_i, \frac{\zeta_1}{\nu^2}\right) f_{i/a}\left(\frac{x_1}{x}, \mu_i\right) + \mathcal{O}(b^2 \Lambda_{\text{QCD}}^2)$$

- **Soft function** (with a staple Wilson line because $S(\mathbf{b}, \mu, \nu) = \frac{1}{N_c} \langle 0 | \text{Tr} [W_{\gg}(\mathbf{b})] | 0 \rangle$)

Evolution and pp example

Modes and scales in TMD DY

$$p_c \sim Q(1, \lambda^2, \lambda), \quad p_{\bar{c}} \sim Q(\lambda^2, 1, \lambda), \quad p_s \sim Q(\lambda, \lambda, \lambda)$$



RG

$$\frac{d}{d \ln \mu} \ln H(Q, \mu) = \gamma_{\mu}^H(Q, \mu),$$

$$\frac{d}{d \ln \mu} \ln B\left(x, b, \mu, \frac{\zeta}{\nu^2}\right) = \gamma_{\mu}^B\left(\mu, \frac{\zeta}{\nu^2}\right),$$

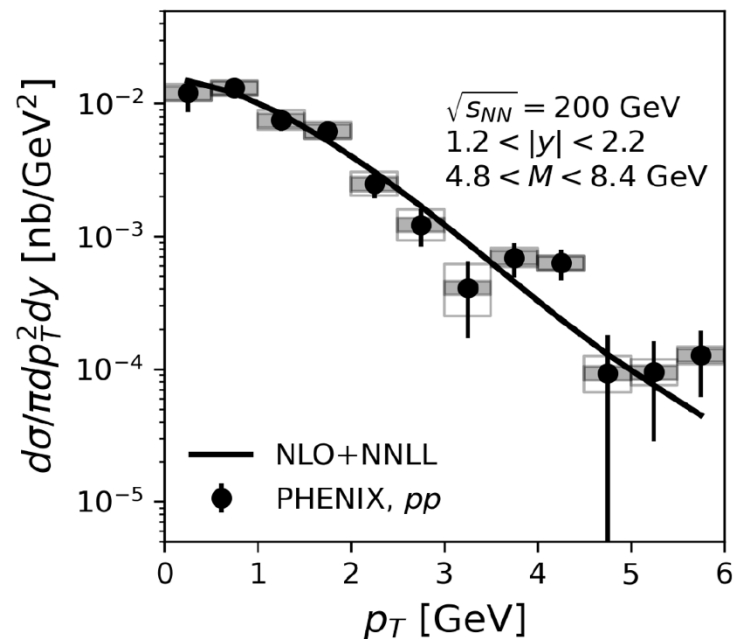
$$\frac{d}{d \ln \mu} \ln S(b, \mu, \nu) = \gamma_{\mu}^S\left(\mu, \frac{\mu}{\nu}\right).$$

RRG

$$\frac{d \ln B}{d \ln \nu} = \gamma_{\nu}^B(b, \mu),$$

$$\frac{d \ln S}{d \ln \nu} = \gamma_{\nu}^S(b, \mu)$$

J. Chiu et al. (2012)



Comparison to the PHENIX data

- Note the emergence of the Collins-Soper scales (CS)

$$\sqrt{\zeta_1} = p_a^+ \text{ and } \sqrt{\zeta_2} = p_b^- \text{ with } \sqrt{\zeta_1 \zeta_2} = Q^2.$$

- Evolution is controlled by renormalization group (RG) and rapidity renormalization group (RRG) equations

NLO+NNLL code with NP effects *M. Alrashed et al. (2021)*

$$S_{\text{NP}}^f(\mathbf{b}, Q) = \frac{g_2}{2} \ln \frac{b}{b^*} \ln \frac{\sqrt{\zeta}}{\sqrt{\zeta_0}} + g_1^f b^2 \quad b^* = \frac{b}{\sqrt{1 + b^2/b_{\text{max}}^2}}, \quad \mu_b^* = 2e^{-\gamma_E}/b^*$$

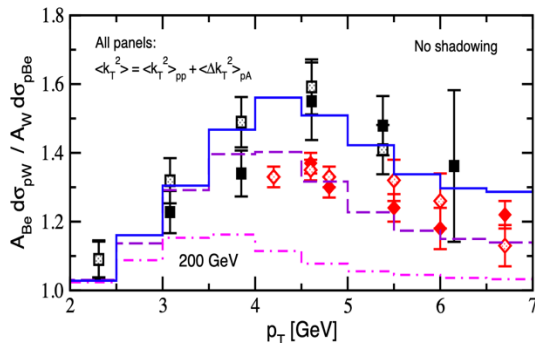
Note that as we go to high p_T we will underpredict the data. Not matched to collinear calculation (the “Y” term)

TMD DY in pA and CNM effects

Our goal is to calculate TMD DY in pA reactions. Understand cold nuclear matter effects that can be calculated perturbatively (at least partly)

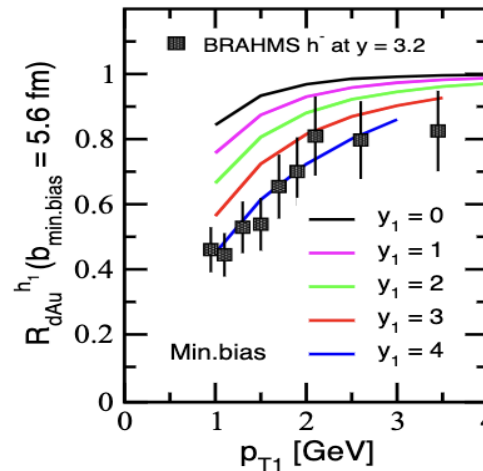
- Some can be of leading twist nature parametrized in nPDFs
W3 talks by P. Duwentaester, J. Terry
- Many can be understood from the coherent, incoherent and inelastic scattering in nuclei

I. Vitev et al. (2002)

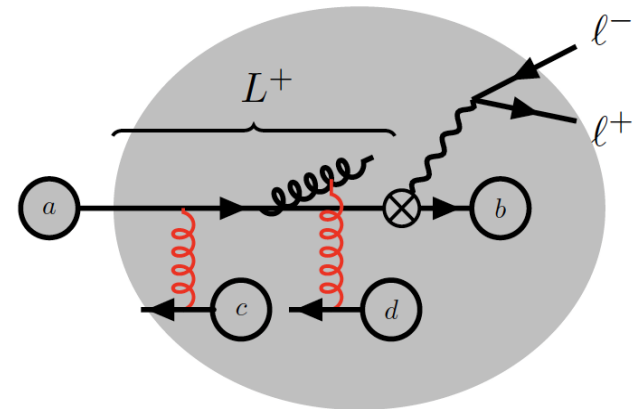


Cronin effect

Goal is to combine in a unified first principles formalism



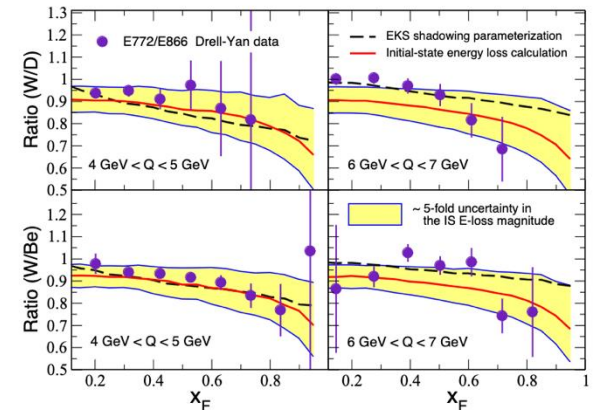
Coherent power corrections



Schematic of DIS in nuclei

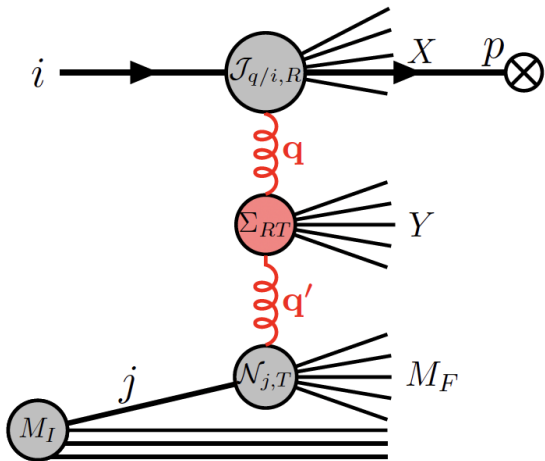
J. Qiu et al. (2005)

B. Neufeld et al. (2010)



Energy loss

Structure of the calculation in matter



Take the opacity expansion approach and calculate the correction to the proton beam function

Factorized expression for first order in opacity correction

$$\mathcal{B}_{q/a} = \mathcal{B}_{q/a,0} + \chi \mathcal{B}_{q/a,1} + \dots$$

$$\frac{d\sigma_1}{dPS} = \frac{4\pi\alpha_{em}^2}{3N_c Q^2 s} H(Q, \mu) \sum_q c_q(Q) \int \frac{d^2\mathbf{b}}{(2\pi)^2} e^{i\mathbf{P}_T \cdot \mathbf{b}} \times \sum_{N \in A} \mathcal{B}_{q/p,1} \left(x_1, b, \mu, \frac{\zeta_1}{\nu^2}; \mu_E, \mathcal{L}_1 \right) \mathcal{B}_{\bar{q}/N} \left(x_2, b, \mu, \frac{\zeta_2}{\nu^2} \right) S(b, \mu, \nu).$$

We further isolate the effects in the partonic scattering cross section and effective Glauber gluon density

$$\mathcal{B}_{q/p,1} = \sum_{i=q,g} \sum_{j=q,\bar{q},g} \sigma_{ij \rightarrow q} \otimes f_{i/p} \otimes f_{j/N} \cdot \rho_0^- L^+$$

Structure of the partonic cross section (quark example)

$$\begin{aligned} \sigma_{q/q,T}^{(0)} + \sigma_{q/q,T}^{(1)} = & \left(\mathcal{J}_{q/q,F}^{(0)} + \mathcal{J}_{q/q,F}^{(1),\text{rap}} \right) \otimes \Sigma_{FT}^{(0)} \otimes \mathcal{N}_T^{(0)} + \\ & \mathcal{J}_{q/q,F}^{(1),\text{coll}} \otimes \Sigma_{FT}^{(0)} \otimes \mathcal{N}_T^{(0)} + \mathcal{J}_{q/q,A}^{(1),\text{coll}} \otimes \Sigma_{AT}^{(0)} \otimes \mathcal{N}_T^{(0)} \\ & \mathcal{J}_{q/q,A}^{(1),\text{rap}} \otimes \Sigma_{AT}^{(0)} \otimes \mathcal{N}_T^{(0)} + \mathcal{J}_{q/q,F}^{(0)} \otimes \Sigma_{FT}^{(1)} \otimes \mathcal{N}_T^{(0)} + \mathcal{J}_{q/q,F}^{(0)} \otimes \Sigma_{FT}^{(0)} \otimes \mathcal{N}_T^{(1)} \\ & + \Delta\sigma_{q/q,T}^{\text{NLO}}, \end{aligned}$$

Fixed order piece

- Tree level terms
- Collinear divergences
- Rapidity divergences
- Soft radiation and anti-collinear

The LPM effect

Before we dive into the calculation, we need to consider coherence in the emission process on a nuclear target

$$\Phi_n = 1 - \frac{\sin\left(\frac{Q_n^2 L^+}{2x(1-x)p_1^+}\right)}{\frac{Q_n^2 L^+}{2x(1-x)p_1^+}} \quad \tau_f = \frac{1}{p^-} = \frac{x(1-x)p^+}{p^2}$$

L. Landau et al. (1953)

A. Migdal (1956)

The non-trivial scales

Long formation times

Short formation times

$$\mu_E \gg \mu_b \quad \ln(\mu_b^2 / \Lambda_{\text{QCD}}^2)$$

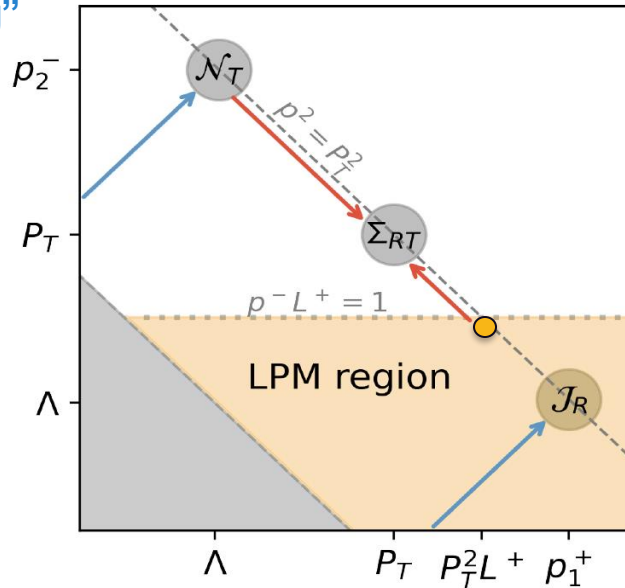
$$\mu_E \ll \mu_b \quad \ln(\mu_E^2 / \Lambda_{\text{QCD}}^2)$$

“Standard scale ordering”

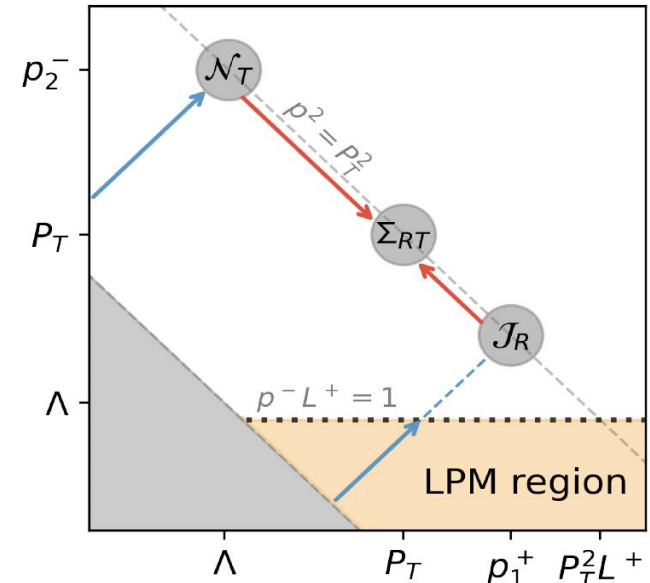
$$\Lambda_{\text{QCD}}^2 \ll \mu_E^2 \ll Q^2$$

$$\sqrt{\zeta_1} / \Lambda_{\text{QCD}}^2 \gg L^+ \gg \sqrt{\zeta_1} / Q^2.$$

- Kinematics suggests that we have dominant contributions from the first scenario
- We consider both and provide formulas that interpolate



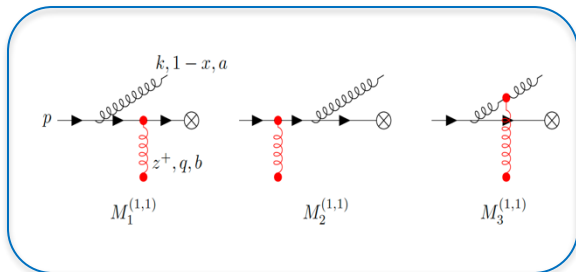
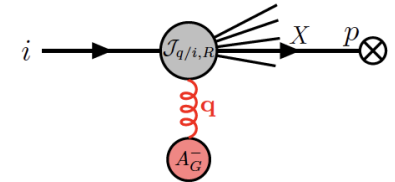
The collinear emission is in the LPM region. Evolution space limited



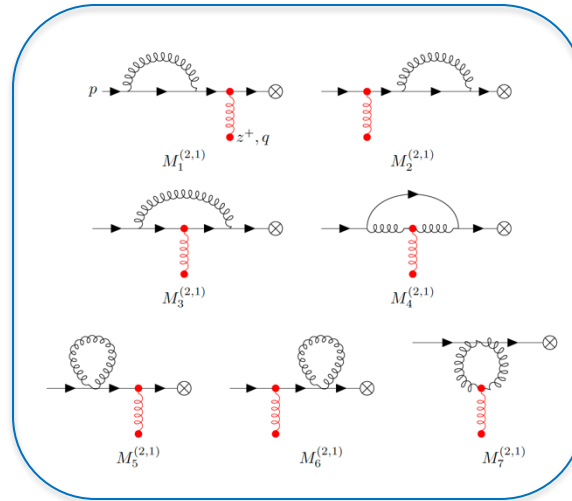
The collinear emission is outside LPM region. Evolution space not limited

Diagrams for the collinear matching coefficient function

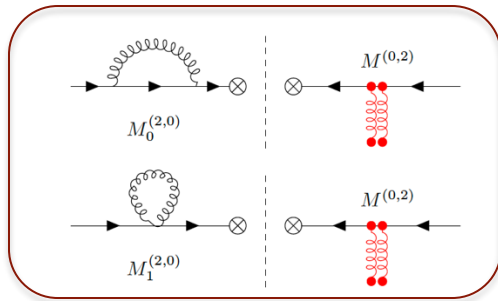
We need to evaluate diagrams that impart transverse momentum via collisions (Glauber gluons) or radiation (or not). SCET_G sufficient



Single Glauber, real radiation

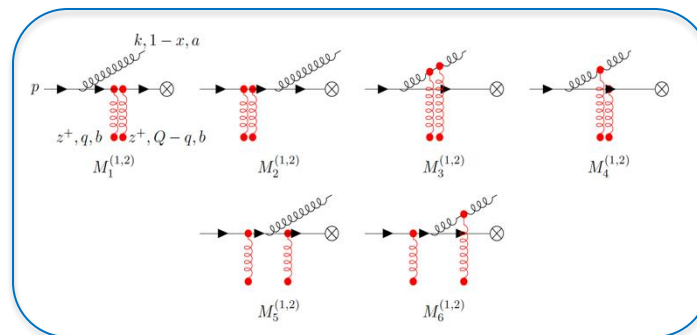


Single Glauber, loop correction

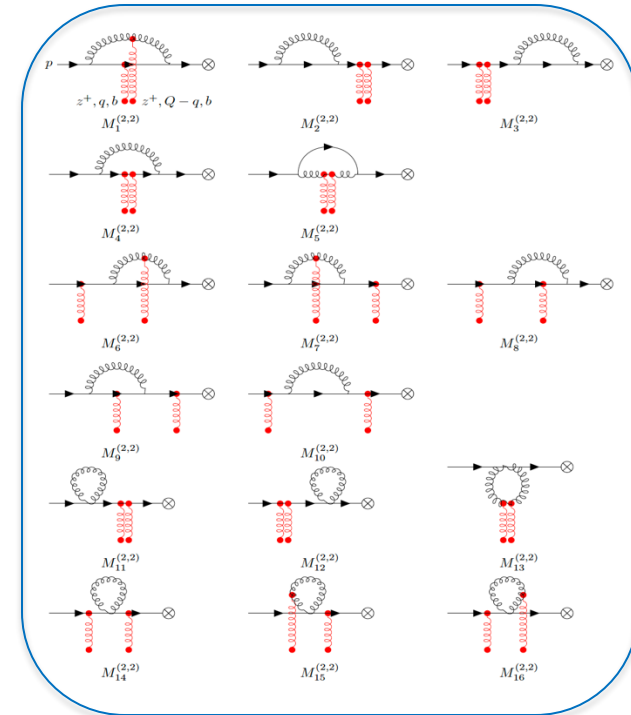


Wavefunction renormalization

Vanishes to leading power (scales integrals)



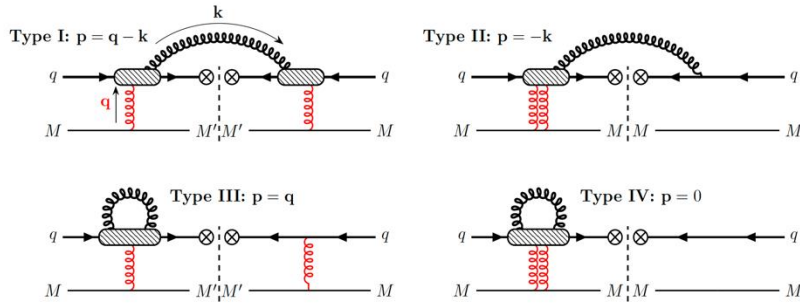
Double Glauber, real radiation



Double Glauber, loop correction

- New direct calculation of loop diagrams

Collinear function results



The 4 classes of diagrams contribute differently to the longitudinal and transverse momentum flow in the DY process

Flavor sum rule explicitly satisfied

$$\int_0^1 dx \int d^2\mathbf{p} \int d^2\mathbf{q} \mathcal{J}_{q/q,R}^{(1)}(x, \mathbf{p}, \mathbf{q}) = 0$$

$$\begin{aligned} \mathcal{J}_{q/q,R}^{(1)}(x, \mathbf{p}, \mathbf{q}) &= \frac{g_s^2 C_F}{2\pi} P_{qq}(x) \int d^2\mathbf{k} \left[\delta^{(2)}(\mathbf{p} - \mathbf{q} + \mathbf{k}) \mathcal{I}_{I,R}(x, \mathbf{p}, \mathbf{q}) + \delta^{(2)}(\mathbf{p} + \mathbf{k}) \mathcal{I}_{II,R}(x, \mathbf{p}, \mathbf{q}) \right] \\ &+ \frac{g_s^2 C_F}{2\pi} \delta(1-x) \int_0^1 dx' P_{qq}(x') \int d^2\mathbf{k} \left[\delta^{(2)}(\mathbf{p} - \mathbf{q}) \mathcal{I}_{III,R}(x', \mathbf{k}, \mathbf{q}) + \delta^{(2)}(\mathbf{p}) \mathcal{I}_{IV,R}(x', \mathbf{k}, \mathbf{q}) \right]. \end{aligned}$$

- With kinematic variable definitions, they are given explicitly and with the LPM effect

$$\mathbf{Q}_1 = x\mathbf{k} - (1-x)(\mathbf{p}_0 - \mathbf{k}),$$

$$\mathbf{Q}_2 = x\mathbf{k} - (1-x)(\mathbf{p}_0 - \mathbf{k} + \mathbf{q}),$$

$$\mathbf{Q}_3 = x(\mathbf{k} - \mathbf{q}) - (1-x)(\mathbf{p}_0 - \mathbf{k} + \mathbf{q}),$$

$$\mathbf{Q}_4 = x(\mathbf{k} + \mathbf{q}) - (1-x)(\mathbf{p}_0 - \mathbf{k}),$$

| Type K | $\mathcal{I}_F^K(x, \mathbf{k}, \mathbf{q})$ | $\mathcal{I}_A^K(x, \mathbf{k}, \mathbf{q})$ |
|----------|---|---|
| I | $\frac{1}{Q_1^2} + 2 \frac{Q_2}{Q_2^2} \cdot \left(\frac{Q_2}{Q_2^2} - \frac{Q_1}{Q_1^2} \right) \Phi_2$ | $\frac{1}{Q_3^2} - \frac{Q_1}{Q_1^2} \cdot \frac{Q_3}{Q_3^2} + \frac{Q_2}{Q_2^2} \cdot \left(\frac{Q_1}{Q_1^2} - \frac{Q_3}{Q_3^2} \right) \Phi_2$ |
| II | $-\frac{1}{Q_1^2}$ | $\frac{Q_1}{Q_1^2} \cdot \left(\frac{Q_1}{Q_1^2} - \frac{Q_3}{Q_3^2} \right) (\Phi_1 - 1)$ |
| III | $-2 \frac{Q_2}{Q_2^2} \cdot \left(\frac{Q_2}{Q_2^2} - \frac{Q_1}{Q_1^2} \right) \Phi_2$ | $-\frac{Q_1 \cdot Q_2}{Q_1^2 Q_2^2} \Phi_2 + \frac{Q_2}{Q_2^2} \cdot \frac{Q_4}{Q_4^2} \Phi_4$ |
| IV | 0 | $-\frac{1}{Q_1^2} \Phi_1 + \frac{Q_1 \cdot Q_5}{Q_1^2 Q_5^2} \Phi_5$ |

- The important part is how to identify and treat collinear and rapidity divergences and derive renormalization group equations

Medium-induced collinear divergences

In this form the results are not quite ready yet for RG analysis

Under dim. reg. on can change variables, perform power expansion and take the transverse integrals

$$\begin{aligned} & \mathcal{J}_{q/q,F}^{(1),\text{coll}} \otimes \Sigma_{FT}^{(0)} \otimes \mathcal{N}_{j,T}^{(0)} + \mathcal{J}_{q/q,A}^{(1),\text{coll}} \otimes \Sigma_{AT}^{(0)} \otimes \mathcal{N}_{j,T}^{(0)} \\ &= \int \frac{d^{2-2\epsilon} \mathbf{q}}{(2\pi)^{2-2\epsilon}} \frac{g_s^2 C_A g_s^2 C_T}{d_A} \frac{1}{\mathbf{q}^4} \int \frac{d^{2-2\epsilon} \mathbf{k}}{(2\pi)^{2-2\epsilon}} g_s^2 \frac{C_F}{2\pi} \left[P_{qq}(x) \left\{ \frac{\mathbf{B}}{\mathbf{B}^2} \cdot \left(\frac{\mathbf{B}}{\mathbf{B}^2} - \frac{\mathbf{C}}{\mathbf{C}^2} \right) \Phi_B \right. \right. \\ & \left. \left. + \frac{\mathbf{C}}{\mathbf{C}^2} \cdot \left(\frac{\mathbf{C}}{\mathbf{C}^2} - \frac{\mathbf{A}}{\mathbf{A}^2} \right) \Phi_C + \left(\frac{2C_F}{C_A} - 1 \right) \frac{\mathbf{B}}{\mathbf{B}^2} \cdot \left(\frac{\mathbf{B}}{\mathbf{B}^2} - \frac{\mathbf{A}}{\mathbf{A}^2} \right) \Phi_B \right\} \right]_+ + \mathcal{O} \left(\frac{\mu_E^2}{\mu_b^2} \right). \end{aligned}$$

Main features of the analytic results

$$\begin{aligned} & \mathcal{J}_{q/q,F}^{(1),\text{coll}} \otimes \Sigma_{FT}^{(0)} \otimes \mathcal{N}_{j,T}^{(0)} + \\ & \mathcal{J}_{q/q,A}^{(1),\text{coll}} \otimes \Sigma_{AT}^{(0)} \otimes \mathcal{N}_{j,T}^{(0)} \supset \frac{\rho_G L \alpha_s^2(\mu^2)}{8p_1^+/L^+} \cdot \left[\frac{\mu^2}{2p^+/L^+} \right]^{2\epsilon} B_\epsilon \left(\frac{\mu_b^2}{2p^+/L^+} \right) \int_0^1 \frac{dx'}{x'} \frac{P_{qq}^{(0)}(x')}{[x'(1-x')]^{1+2\epsilon}} f_{q/p} \left(\frac{x}{x'} \right) \times [\text{Color factors}] \\ &= \frac{\alpha_s^2(\mu^2) B_0(\mu_b^2 L/2p^+) \rho_G L}{8p^+/L^+} \left(\frac{1}{2\epsilon} + \ln \frac{\mu^2}{\min\{\mu_b^2, 2p^+/L^+\}} \right) 2C_F \left[2C_A \left(-\frac{d}{dz} + \frac{1}{z} \right) + \frac{C_F}{z} \right] z f_q(z) \end{aligned}$$

- In medium radiation leads to additional $1/x(1-x)$ divergences at the endpoints of the splitting functions
- This can be handled by a generalized + prescription (that now includes derivatives of the function at the endpoints)
- One sees the emergence of the in-medium logarithms and a pole that can be canceled by a counter term

Can be a separate topic in itself

See W. Ke et al. (2023), talk in W2 I. Vitev

In-medium collinear RG evolution

- Derived a full new set of RG evolution equations. The NS distribution has a very elegant traveling wave solution

Suitable change of variables. Also captures the density, path length and energy dependence

$$\tau(\mu^2) = \frac{B(w)\rho_G^- L^+}{8p_1^+ / L^+} \frac{4\pi}{\beta_0} \left[\alpha_s(\mu^2) - \alpha_s \left(\frac{\gamma(w)p_1^+}{L^+} \right) \right]$$

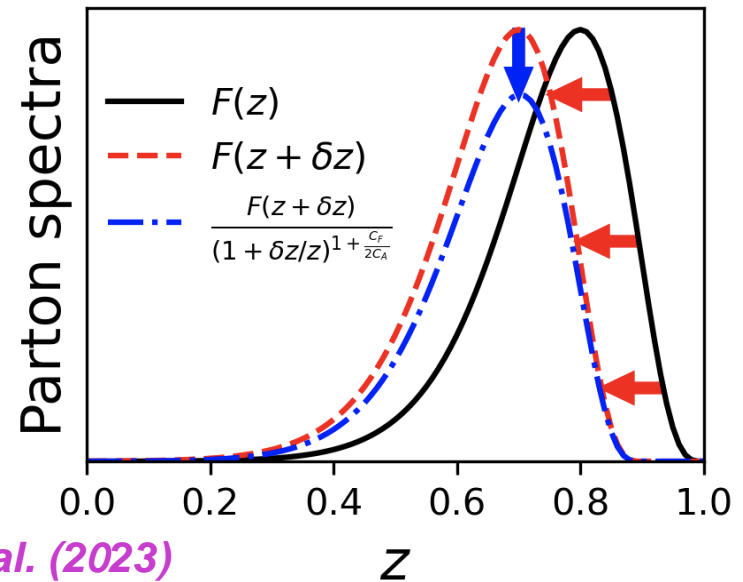
Flavor non-singlet (q-qbar) Flavor singlet (q+qbar, g)

$$\frac{\partial F_{q-\bar{q}}}{\partial \tau} = \left(4C_F C_A \frac{\partial}{\partial x} - \frac{4C_F C_A}{x} - \frac{2C_F^2}{x} \right) F_{q-\bar{q}}$$

$$\frac{\partial F_{q+\bar{q}}}{\partial \tau} = \left(4C_F C_A \frac{\partial}{\partial x} - \frac{4C_F C_A}{x} - \frac{2C_F^2}{x} \right) F_{q+\bar{q}} + \frac{2C_F T_F}{x} F_g,$$

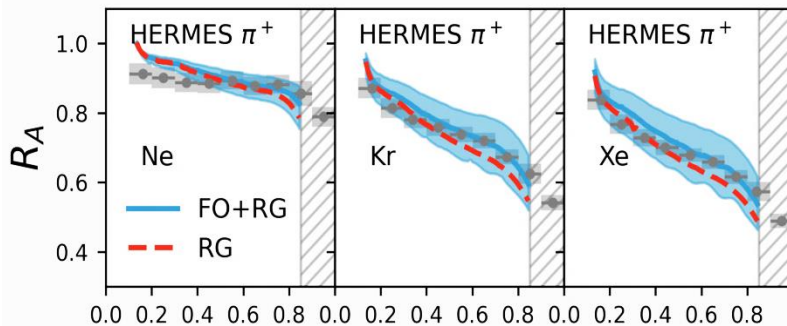
$$\frac{\partial F_g}{\partial \tau} = \left(4C_A^2 \frac{\partial}{\partial x} - \frac{2N_f C_F}{x} \right) F_g + \sum_q \frac{2C_F^2}{x} F_{q+\bar{q}}.$$

$$F_{\text{NS}}(\tau, z) = \frac{F_{\text{NS}}(0, z + 4C_F C_{AT})}{(1 + 4C_F C_{AT}/z)^{1+C_F/(2C_A)}}$$



W. Ke et al. (2023)

Can directly identify parton energy loss, the nuclear size dependence of the modification, etc



- Connection to EIC: The same in-medium RG evolution describes the suppression of hadron production in SIDIS on nuclei

The TMD parton energy loss

- We can identify the **energy loss of the parton** (driven by soft emission)

$$\Delta p_1^+ \Big|_{\mu_E \ll \mu_b} = \frac{B(w) \rho_G^-(L^+)^2}{8} \frac{4\pi}{\beta_0} [\alpha_s(\xi^2) - \alpha_s(\gamma(w) \mu_E^2)]$$

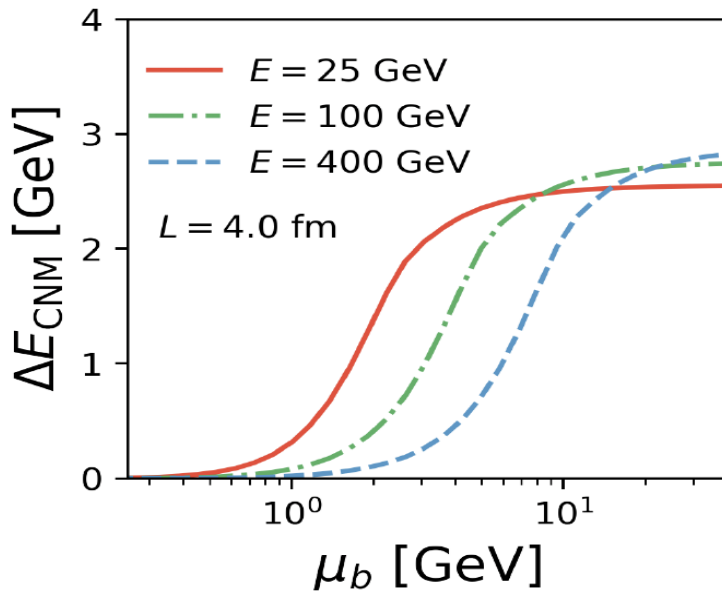
$$\Delta p_1^+ \Big|_{\mu_b \ll \mu_E} \approx \frac{2}{3\pi} \frac{\mu_b^2}{\mu_E^2} \frac{\rho_G^-(L^+)^2}{8} \frac{4\pi}{\beta_0} [\alpha_s(\xi^2) - \alpha_s(2e^{-1} \mu_b^2)]$$

Because $B(w \ll 1) \approx \frac{2}{3\pi} \frac{\mu_b^2}{\mu_E^2}$, $\gamma(w \ll 1) \approx \frac{2}{e} \frac{\mu_b^2}{\mu_E^2}$.

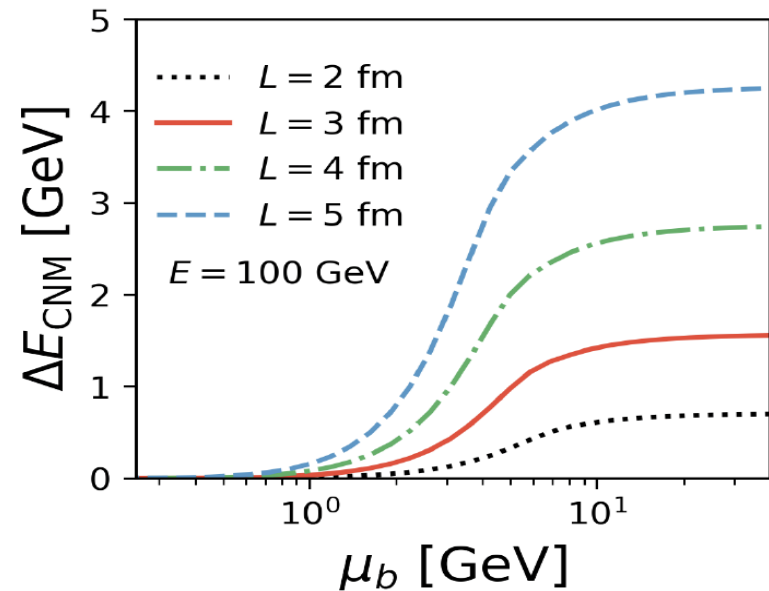
With the functions

$$B(w) = \frac{4}{\pi} \int_0^w \Phi(x) \frac{dx}{x^2}, \quad w = \mu_b^2 / \mu_E^2,$$

$$\gamma(w) = 2 \exp \left\{ \frac{1}{B(w)} \frac{4}{\pi} \int_0^w \Phi(x) \ln(x) \frac{dx}{x^2} \right\}$$



E-loss vs energy



E-loss vs size

Rapidity divergences

Collinear radiation can also lead to rapidity divergences

- Regulated by the η regulator. Rapidity divergences appear as $1/\tau$ poles

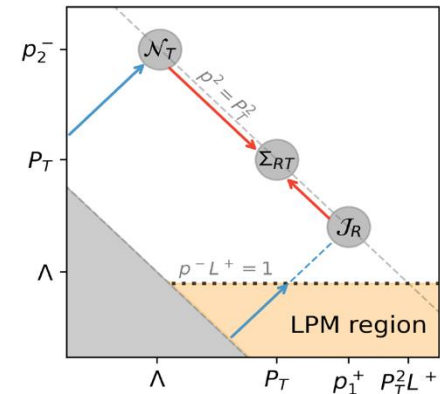
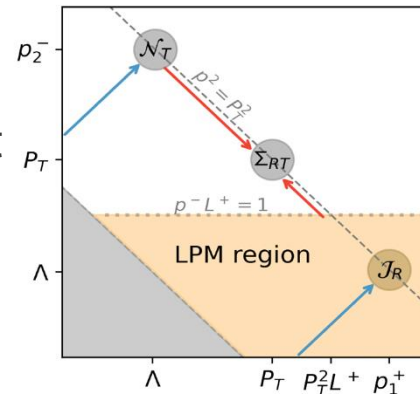
$$\eta(x) = \left(\frac{(1-x)p_1^+}{\nu} \right)^{-\tau}$$

η regulator

$$\mathcal{J}_{q/q,A}^{(1),\text{rap}} \otimes \Sigma_{AT}^{(0)} \otimes \mathcal{N}_T^{(0)} = \delta(1-x) \left[-\frac{1}{\tau} + \mathcal{L}_n + \mathcal{O}(\tau) \right] \int \frac{d^{2-2\epsilon} \mathbf{q}}{(2\pi)^{2-2\epsilon}} \hat{\mathcal{C}} \left[\frac{e^{-i\mathbf{q}\cdot\mathbf{b}}}{\mathbf{q}^2} \right] \mathbf{q}^2 \frac{d\sigma_{FT}^{(0)}}{d^2 \mathbf{q}},$$

- The LPM effect leads to the appearance of a new Collins-Soper (CS) scale $\sim \mu_b^2 L^+ / 2$. The LPM effect on RG and RRG complementary
- The rapidity logarithm becomes

$$\mathcal{L}_n = \ln \frac{\min\{2L^+ \mu_b^2, x_1 P_a^+\}}{\nu}$$



We see the appearance of the BFKL kernel [with action defined on $v(\mathbf{q}^2)$]

$$\hat{\mathcal{C}}[v(\mathbf{q}^2)] = \frac{g_s^2 C_A}{\pi} \int \frac{d^{2-2\epsilon} \mathbf{k}}{(2\pi)^{2-2\epsilon}} \left[\frac{1}{(\mathbf{q} - \mathbf{k})^2} v(\mathbf{k}^2) - \frac{\mathbf{q}^2}{2\mathbf{k}^2(\mathbf{q} - \mathbf{k})^2} v(\mathbf{q}^2) \right]$$

To cancel the rapidity logarithm we need to consider the soft emission from the Glauber scattering and the target ant-collinear sector

Contributions with rapidity divergences

NLO correction to the Glauber cross section $\Sigma^{(1)}$

We consider soft gluon emission

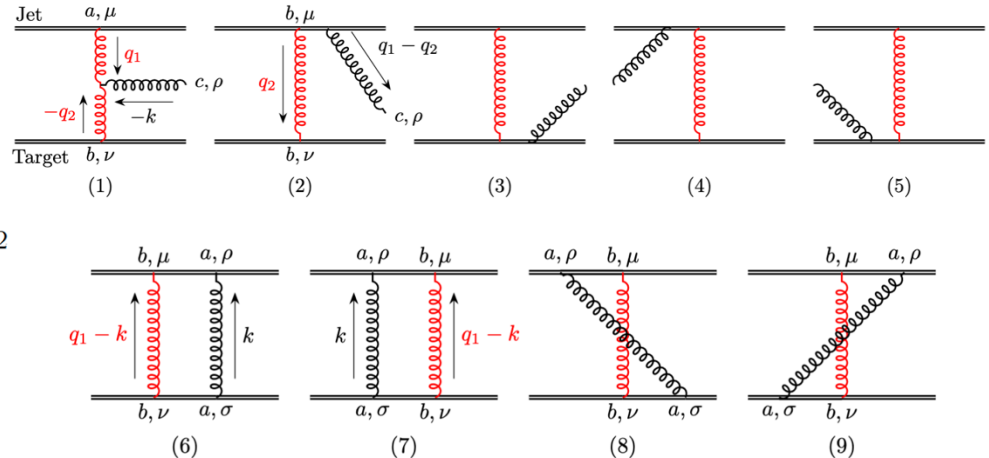
$$k^\mu \sim (\lambda, \lambda, \lambda) \quad \left| \frac{k_z}{\nu} \right|^{-\tau/2} = \left| \frac{k^+ - k^-}{2\nu} \right|^{-\tau/2}$$

- There are other diagrams that look like Glauber self energies and wavefunction renormalization. **Do not contain** rapidity divergences

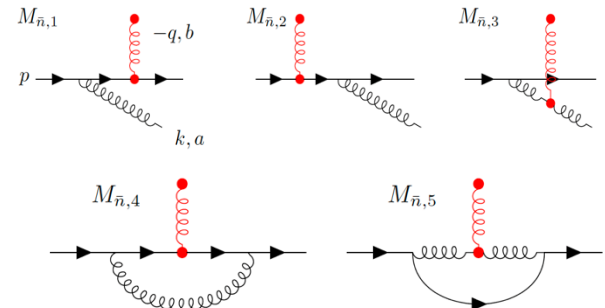
$$\mathcal{J}_{q/q,F}^{(0)} \otimes \Sigma_{FT}^{(1)} \otimes \mathcal{N}_T^{(0)} = \int \frac{d^{2-2\epsilon} \mathbf{p}}{(2\pi)^{-2\epsilon}} e^{-i\mathbf{p}\cdot\mathbf{b}} \int \frac{d^{2-2\epsilon} \mathbf{q}}{(2\pi)^{2-2\epsilon}} \int \frac{d^{2-2\epsilon} \mathbf{q}'}{(2\pi)^{2-2\epsilon}} \frac{\mathcal{J}_{q/q,F}^{(0)}}{\mathbf{q}^2} \left(\frac{2}{\tau} + \mathcal{L}_s \right) \hat{\mathcal{C}} \left[\mathbf{q}^2 \mathbf{q}'^2 \Sigma_{FT}^{(0)} \right] \frac{\mathcal{N}_T^{(0)}}{\mathbf{q}'^2}$$

- Observe the BFKL kernel, pole, and a different soft logarithm $\mathcal{L}_s = \ln \frac{\nu^2}{\mu_b^2}$

NLO correction from the anti-collinear sector $\mathcal{N}_T^{(1)}$



Real and virtual diagrams that contain rapidity divergence



Note that real emission diagrams contribute. These are not the partons in the large Q process. Double Glauber will not put them off-shell

Cancelation of the rapidity divergences

Putting all sectors together we find that

- The $1/\tau$ poles have cancelled
- The logarithms have combined to become

$$\begin{aligned} & \mathcal{J}_{q/q,F}^{(0)} \otimes \Sigma_{FT}^{(1)} \otimes \mathcal{N}_T^{(0)} + \mathcal{J}_{q/q,A}^{(1,\text{rap})} \otimes \Sigma_{AT}^{(0)} \otimes \mathcal{N}_T^{(0)} \\ & + \mathcal{J}_{q/q,F}^{(0)} \otimes \Sigma_{FT}^{(1)} \otimes \mathcal{N}_T^{(0)} + \mathcal{J}_{q/q,F}^{(0)} \otimes \Sigma_{FT}^{(0)} \otimes \mathcal{N}_T^{(1)} \\ & = \delta(1-x) \frac{g_s^2 C_F g_s^2 C_T}{d_A} \int \frac{d^{2-2\epsilon} \mathbf{q}}{(2\pi)^{2-2\epsilon}} e^{i\mathbf{q}\cdot\mathbf{b}} \frac{1}{\mathbf{q}^2} \left[1 + \mathcal{L}_1 \hat{C} \right] \frac{1}{\mathbf{q}^2}. \end{aligned}$$

$$\mathcal{L}_1 = \ln \left(\min \left\{ 4x_t m_N L, \frac{x_1 x_t s}{\mu_b^2} \right\} \right) = \ln \left(\min \left\{ 4m_N L, \frac{x_1 s}{\mu_b^2} \right\} \right) + \ln x_t$$

More thought should be given for phenomenological studies

We can write down the the BFKL-type evolution for the cross section components

$$\frac{g_s^2}{\mathbf{q}^2} \frac{\partial \mathcal{J}_R(x, \mathbf{p}, \mathbf{q}; \nu)}{\partial \ln \nu} = -\hat{C} \left[\frac{g_s^2}{\mathbf{q}^2} \mathcal{J}_R(x, \mathbf{p}, \mathbf{q}; \nu) \right], \quad \text{Keep at their scales}$$

$$\frac{g_s^2}{\mathbf{q}'^2} \frac{\partial \mathcal{N}_T(\mathbf{q}'; \nu')}{\partial \ln \nu'} = -\hat{C} \left[\frac{g_s^2}{\mathbf{q}'^2} \mathcal{N}_T(\mathbf{q}'; \nu') \right], \quad \text{Put all BFKL evolution in the } \Sigma$$

$$\left(\frac{g_s^2}{\mathbf{q}^2} \right)^{-1} \left(\frac{g_s^2}{\mathbf{q}'^2} \right)^{-1} \frac{\partial \Sigma_{RT}(\mathbf{q}, \mathbf{q}'; \nu, \nu')}{\partial \ln \nu} = \hat{C} \left[\left(\frac{g_s^2}{\mathbf{q}^2} \right)^{-1} \left(\frac{g_s^2}{\mathbf{q}'^2} \right)^{-1} \Sigma_{RT}(\mathbf{q}, \mathbf{q}'; \nu, \nu') \right]$$

- A similar equation can be written in ν' for the target

$$\text{from } \nu = \min\{2L^+ \mu_b^2, x_1 P_a^+\} \ (\nu' = x_t P_b^-) \text{ to } \nu = \mu_b \ (\nu' = \mu_b)$$

BFKL equations solver

Used our own numerical BFKL equation solver in impact parameter space

$$\frac{\partial \tilde{v}(\mathbf{b}, \mu)}{\partial y} = \frac{\alpha_s(\mu^2) C_A}{\pi} \left(\tilde{v}(\mathbf{b}, \mu) \ln R^2 + \int_{|\mathbf{b}-\mathbf{b}'| > R|\mathbf{b}|} \frac{d^2 \mathbf{b}'}{\pi} \frac{\tilde{v}(\mathbf{b}', \mu)}{|\mathbf{b} - \mathbf{b}'|^2} + \int_{|\mathbf{b}-\mathbf{b}'| < R|\mathbf{b}|} \frac{d^2 \mathbf{b}'}{\pi} \frac{\tilde{v}(\mathbf{b}', \mu) - \tilde{v}(\mathbf{b}, \mu)}{|\mathbf{b} - \mathbf{b}'|^2} \right),$$

One needs to introduce **separation parameter R** as we have integration over \mathbf{b}'
Can be shown that the result **does not** depend on R

W. Ke et al. (2024)

- Initial condition that interpolates between the vacuum case and the medium case

$$\tilde{v}_T(\mathbf{b}; y=0) = 2\pi \frac{\alpha_s(\mu_b^2 + \xi^2) C_T}{\pi} K_0 \left(b \sqrt{\mu_b^2 + \xi^2} \right)$$

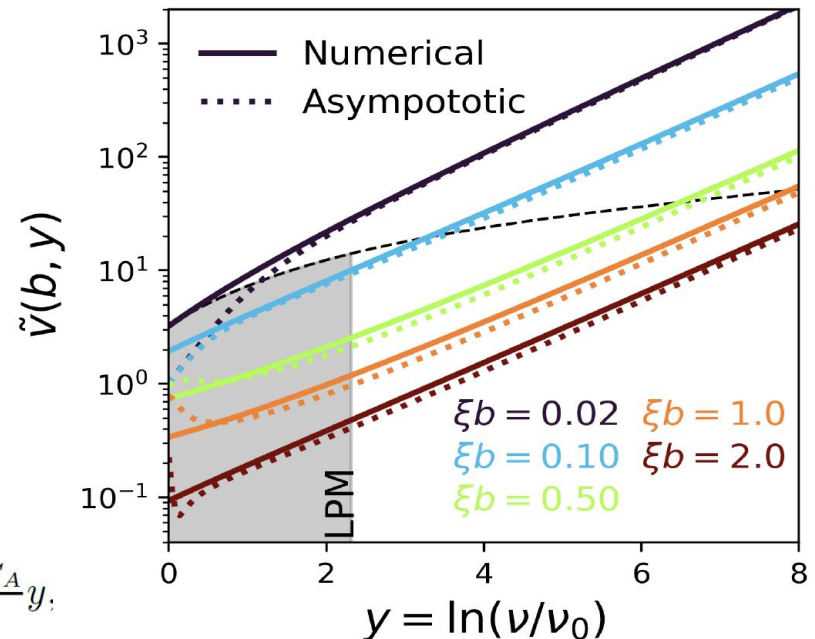
Matched to the DLA initial condition ($y=0$) at $\xi b=0.35$

Analytic solution comparison in the DLA approximation

$$\tilde{v}_T^{\text{DLA}}(\mathbf{b}; y) = C_0 e^{(\alpha_P - 1)y} \int \frac{d^2 \mathbf{q}}{(2\pi^2)} \frac{e^{-i\mathbf{b}\cdot\mathbf{q}}}{2|\mathbf{q}|\xi} \frac{e^{-\frac{[\ln|\mathbf{q}| - \ln \xi]^2}{2\sigma^2 y}}}{\sqrt{2\pi\sigma^2 y}}$$

Parameters $\alpha_P - 1 = \frac{\alpha_{s,\text{fix}} C_A}{\pi} 4 \ln 2, \quad \sigma = 7\zeta(3) \frac{\alpha_{s,\text{fix}} C_A}{\pi} y,$

- Matches well after a few units in rapidity.
Loses memory of initial conditions



BFKL solution compared to the asymptotic case

The final result

Modified p beam function

$$\mathcal{B}_{q/a}^{\text{CNM}} \left(x_1, b, \mu, \frac{\zeta_1}{\nu^2}; \mu_E, \mathcal{L}_1 \right) = \sum_i \int_{x_1}^1 \frac{dx}{x} f_{i/a} \left(\frac{x_1}{x}, \mu_b^*, \mu_E \right) C_{q/i} \left(x, b, \mu_b^*, \frac{\zeta_1}{\nu^2} \right) e^{-S_{\text{NP}}^f(b, \zeta_1)}$$

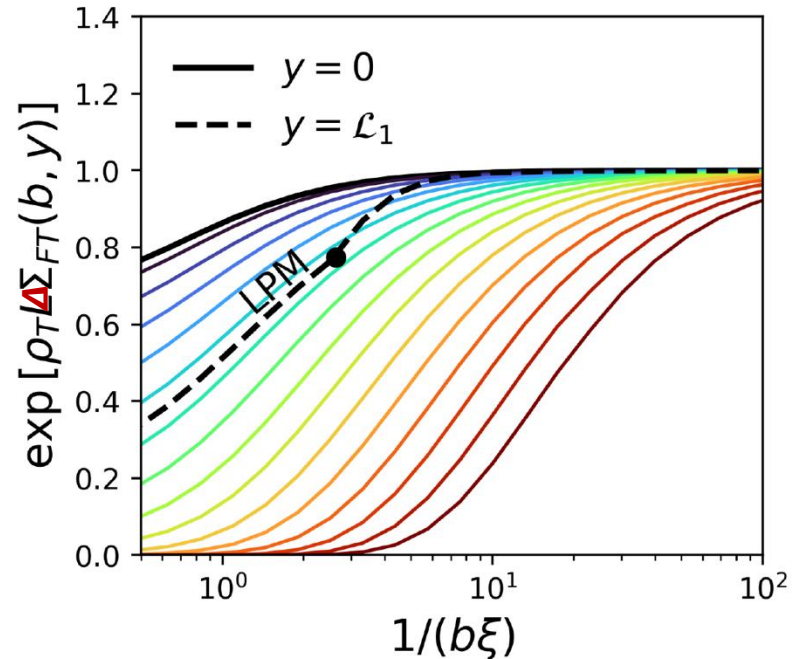
$$\times \exp \left\{ \rho_0^- L^+ \sum_j \int dx_t f_{j/N}(x_t) \left[\tilde{\Sigma}_{ij}(b, \mathcal{L}_1) - \tilde{\Sigma}_{ij}(0, \mathcal{L}_1) \right] \right\}$$

$$\times \left(1 + \rho_0^- L^+ \sum_j \int dx_t f_{j/N}(x_t) \Delta \sigma_{ij \rightarrow q}^{\text{NLO}} \right).$$

- Collinear evolution (RG) modifies the PDF in the proton (including LPM).
- Multiple Glauber gluons exponentiate (including unitarity corrections)
- Radiation enhances broadening, renormalizes (RRG) the forward scattering cross section.
- There are finite contributions

Rapidity evolution of the forward scattering in impact parameter space. Solid line is the boundary condition from tree level Glauber exchange, dashed – the physical boundary.

Broadening ↓



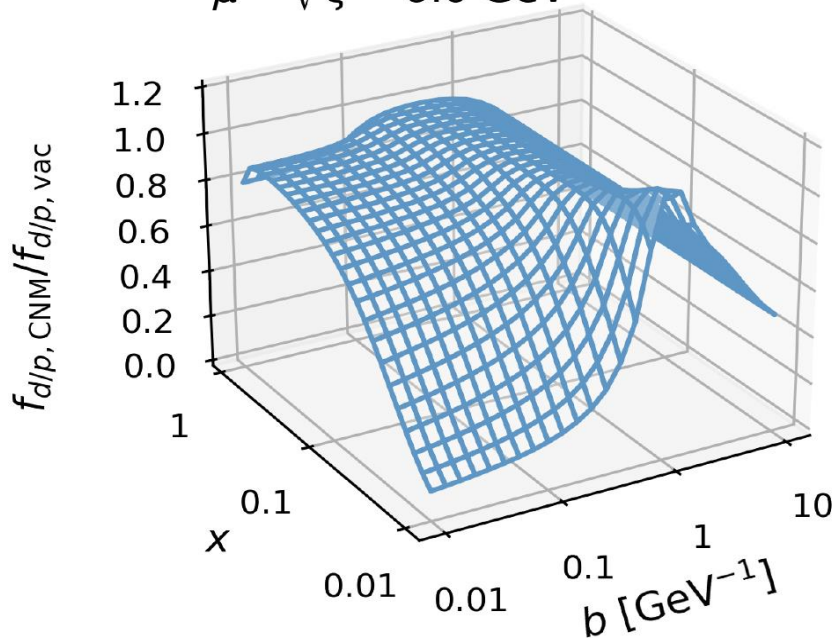
Effective modification of the TMD distribution in pA

- Rich structure appears from CNM effects in 3D proton beam function. Note that scales are set differently then in collinear factorization and reflected on results
- Will affect significantly global extraction

M. Alrashed et al. (2021)

$$\sqrt{s} = 40 \text{ GeV}, L = 5.0 \text{ fm}$$

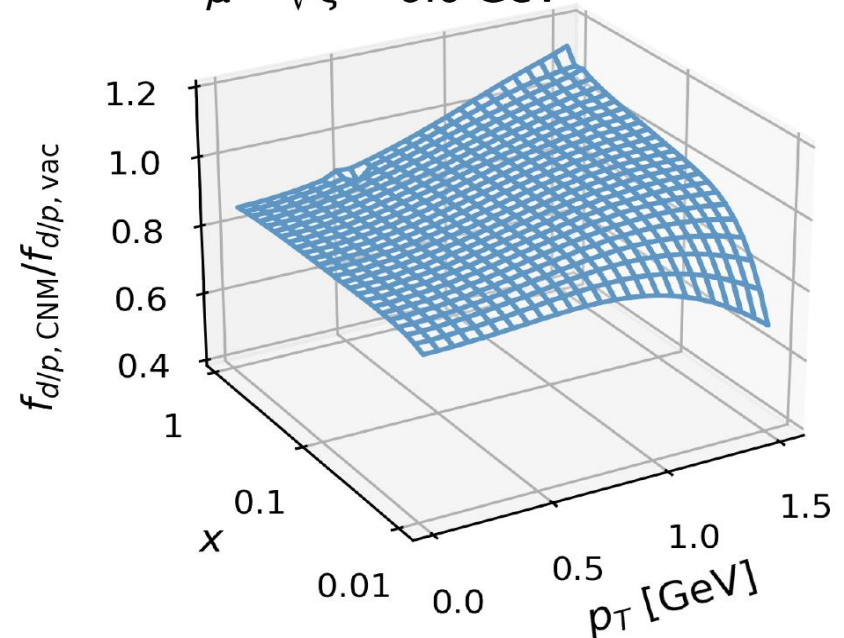
$$\mu = \sqrt{\zeta} = 6.0 \text{ GeV}$$



Impact parameter space

$$\sqrt{s} = 40 \text{ GeV}, L = 5.0 \text{ fm}$$

$$\mu = \sqrt{\zeta} = 6.0 \text{ GeV}$$



Momentum space

One has to be careful pushing to $x \sim 0.01$ and below as one enters a regime of coherent scattering with the target that we did not explicitly consider

Phenomenological results – collider energies and PHENIX data

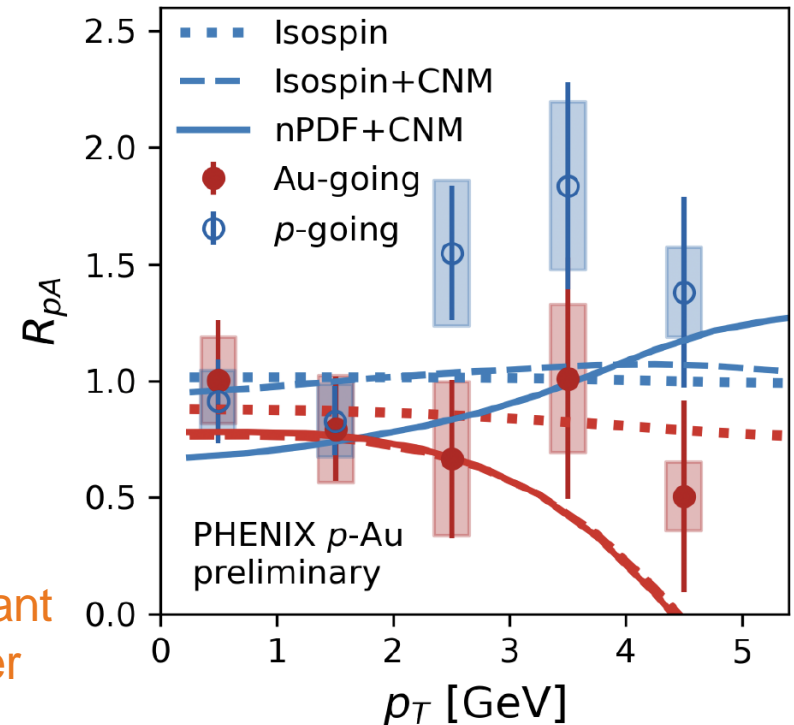
Look at the nuclear modification factor for DY production at small transverse momenta

$$R_{pA} = \frac{1}{A} \frac{d\sigma_{pA}/dQ^2 dy dp_T}{d\sigma_{pp}/dQ^2 dy dp_T}$$

- Isospin gets a little separation in R_{pA} for forward and backward rapidities
- Collisional broadening and radiation lead to further separation
- Including nPDF at scale p_T has an effect on the R_{pA} shape
- Not clear if shape or norm is more important
- When we go to backward rapidity we enter a region of scales where the calculation breaks
- There is no Y term to match at high p_T and scale setting

The error bars have remained quite large in this measurement. Look at more precise fixed target measurements from Fermilab

W. Ke et al. (2024)



Comparison to PHENIX data (which has remained preliminary for quite some time)

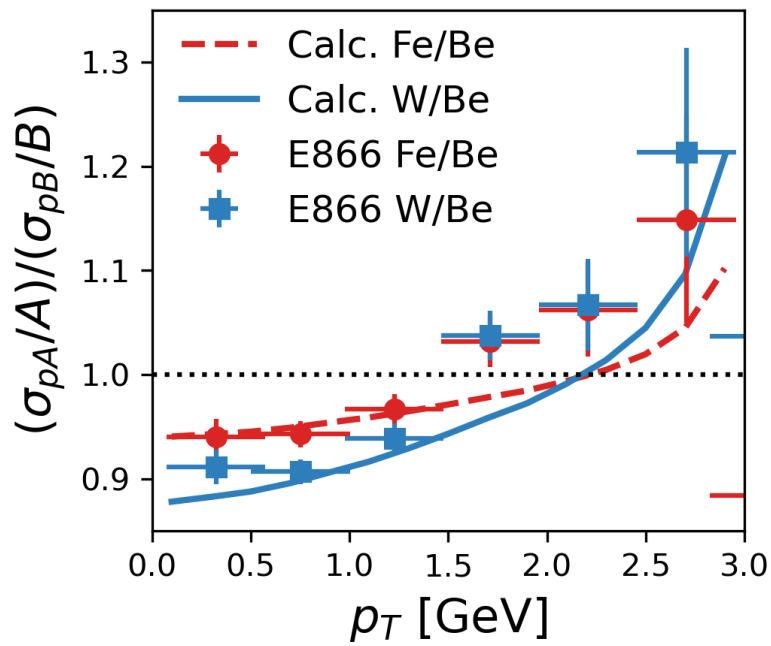
Y. Leung et al. (2019)

Phenomenological results – fixed target energies and E866 data

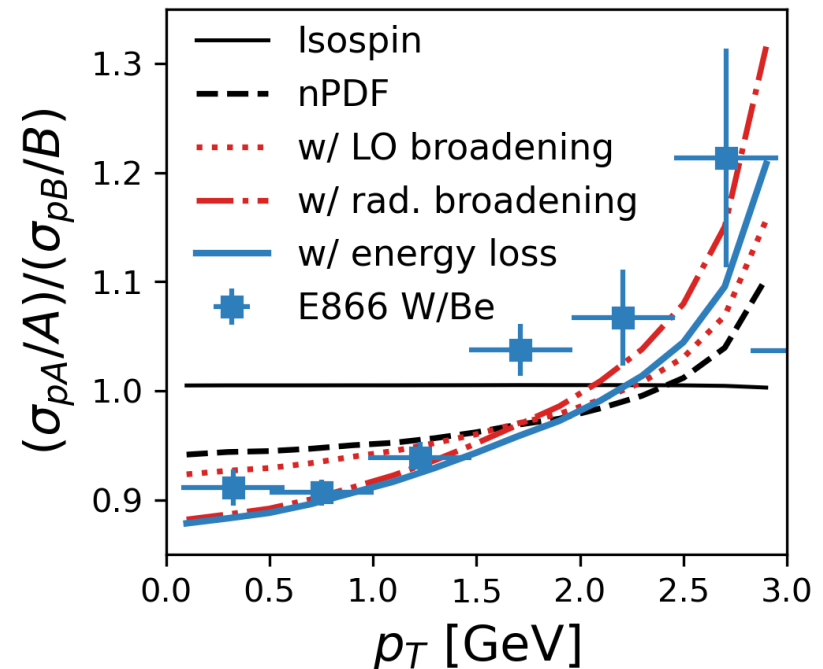
Fixed target experiment data E866 provides ratios of nuclear targets

- The calculation captures the mass dependence
- The nuclear effects derived here are important for a better description of the transition from suppression to enhancement
- Opens the door to phenomenology

M. Vasiliev et al. (1999)



Nuclear size dependence



Contribution of various effects

Conclusions

- TMD physics opens new windows on the structure of hadrons and nuclei, QCD dynamics, and (cold) nuclear matter effects. Resummation of large nuclear matter induced logarithms is essential to interpret the results of reactions with nuclei.
- We focused on DY TMD physics (to complement and orthogonalize to) earlier SIDIS collinear studies. Performed a first principles and self-consistent calculation using SCET with Glauber gluons of TMD DY in pA that combines broadening and radiation effects
- We derived renormalization group (RG) and rapidity renormalization group equations (RRG) that take into account the LPM effect. This provides analytic insights that thus far have been absent in the field (and develops techniques)
- The RG evolution allow to understand parton energy loss, and in this case it is for the TMD framework. Makes connection with the EIC
- The RRG evolution equations also derived, of BFKL type. Numerical solver developed and tested against analytic solutions
- With partial exponentiation to higher orders in opacity applied to phenomenology. Partial success, but also identifying the limitations and direction for future, from scale setting, to better understanding the rapidity log and matching to the collinear formalism

Thank you